Odor vapor pressure and quality modulate local field potential oscillatory patterns in the olfactory bulb of the anesthetized rat

Tristan Cenier,[1] Corine Amat,[1] Philippe Litaudon,[1] Samuel Garcia,[1] Pierre Lafaye de Micheaux,[2,3] Benoît Liquet,[2] Stéphane Roux[4] and Nathalie Buonviso[1]

[1]Neurosciences Sensorielles, Comportement, Cognition, CNRS UMR5020, IFNL, Université Claude Bernard Lyon 1, 50 avenue Tony Garnier, 69366 Lyon cedex 07, France
[2]Université Pierre Mendès France, Département de Statistique du Laboratoire Jean Kuntzman, Grenoble, France
[3]Institut des Neurosciences de Grenoble, Grenoble, France
[4]Laboratoire de Physique, Ecole Normale Supérieure de Lyon, Lyon, France

Abstract

A central question in chemical senses is the way that odorant molecules are represented in the brain. To date, many studies, when taken together, suggest that structural features of the molecules are represented through a spatio-temporal pattern of activation in the olfactory bulb (OB), in both glomerular and mitral cell layers. Mitral/tufted cells interact with a large population of inhibitory interneurons resulting in a temporal patterning of bulbar local field potential (LFP) activity. We investigated the possibility that molecular features could determine the temporal pattern of LFP oscillatory activity in the OB. For this purpose, we recorded the LFPs in the OB of urethane-anesthetized, freely breathing rats in response to series of aliphatic odorants varying subtly in carbon-chain length or functional group. In concordance with our previous reports, we found that odors evoked oscillatory activity in the LFP signal in both the beta and gamma frequency bands. Analysis of LFP oscillations revealed that, although molecular features have almost no influence on the intrinsic characteristics of LFP oscillations, they influence the temporal patterning of bulbar oscillations. Alcohol family odors rarely evoke gamma oscillations, whereas ester family odors rather induce oscillatory patterns showing beta/gamma alternation. Moreover, for molecules with the same functional group, the probability of gamma occurrence is correlated to the vapor pressure of the odor. The significance of the relation between odorant features and oscillatory regimes along with their functional relevance are discussed.

Introduction

The olfactory epithelium contains a large panel of olfactory receptors that can number up to 1000 in some rodent species (Buck & Axel, 1991). At the molecular level, each olfactory receptor is tuned to one particular structural feature of a molecule (Zhao et al., 1998; Malnic et al., 1999; Hallem & Carlson, 2006). Olfactory sensory neurons expressing the same olfactory receptor project their axons onto one or very few glomeruli in the olfactory bulb (OB) (Vassar et al., 1994; Mombaerts et al., 1996; Mori et al., 2006). Thus, specific odor stimulations will elicit specific patterns of glomerular activation. This has been confirmed by studies based on several techniques, such as optical imaging (Rubin & Katz, 1999; Uchida et al., 2000; Belluscio & Katz, 2001) or 2-deoxyglucose uptake (Jourdan et al., 1980; Johnson et al., 1998).

Many consider the glomerulus to be the entry point into an activity-dependent functional organized in columns (Buonviso & Chaput, 1990; Buonviso et al., 1992; Willhite et al., 2006). One would therefore expect a reproduction of the glomerular spatial map onto the mitral/tufted cell layer. Consistent with this view, Mori's group showed that individual mitral/tufted cells respond to a range of odors that share a specific combination of molecular features (Imamura et al., 1992; Mori et al., 1992; Katoh et al., 1993). However, the secondary dendrites of mitral/tufted cells extend over long distances in the external plexiform layer. This extension allows mitral/tufted cells from distant glomeruli to communicate via reciprocal synapses on granular interneurons (Rall et al., 1966; Mori et al., 1983; Shepherd & Greer, 1998).

This vast network of synaptic connections is thought to result in the temporal patterning of the local field potential (LFP) signal. This LFP signal received increasing attention as the potential role of its underlying mechanisms in information coding was revealed (Wehr & Laurent, 1996; Friedrich & Laurent, 2001). Indeed, oscillations of the LFP signal are correlated to the transient synchronization of a population of neurons, a phenomenon that has been shown to be functionally relevant for the discrimination of closely related odorants (Stopfer et al., 1997). Modifications of LFP patterns also seem to reflect memorization and learning (Martin et al., 2004). In mammals, bulbar LFPs and breathing are closely related (Buonviso et al., 2003), suggesting that LFPs are partially driven by the bulbar afferent input. In such conditions, it can be expected that odor molecular features will

Correspondence: Dr Tristan Cenier, as above.
E-mail: tcenier@olfac.univ-lyon1.fr

influence bulbar LFP signals by determining bulbar spatio-temporal input patterns. To our knowledge, it has not yet been shown that different molecular features can differentially affect the LFP bulbar signal in an anesthetized animal.

In this study, we systematically analysed the characteristics of the LFPs evoked by similar or dissimilar aliphatic, straight-chain chemicals with variations in either carbon-chain length (L) or functional group (F). Our goal was to find out if odor quality could influence the temporal pattern of LFP oscillatory activity in the OB.

Materials and methods

Preparation and recording apparatus

Experiments were performed on freely breathing, anesthetized male Wistar rats weighing 200–300 g (Charles River Laboratories, L'Arbresle, France). Anesthesia was performed through an intraperitoneal injection of urethane (1.5 g/kg). Supplemental doses were delivered during experimentation when necessary. All surgical procedures were conducted in strict accordance with the European Community Council guidelines. Animals were immobilized with ear and teeth bars in a stereotaxic apparatus. The skull was exposed and a small bone window was drilled above the OB to grant full access to its dorsal aspect. Neuronal activity was recorded within the mitral cell layer using a 16-channel silicon neural probe (Neuronxus Technologies). The 16 recording points were dispatched linearly along the silicone tip at 50 μm intervals. The electrode was lowered vertically along the dorso-ventral axis and the bulb entry point was chosen so that most of the recording points lay near the mitral cell layer. In an effort to avoid spatial odor-specific glomerular activation effects, recording sites were dispatched along the entire antero-posterior axis of the OB and the entire dorso-ventral axis of the lateral and medial layers. The extracellular signal was acquired in the full band (0–5000 Hz) and digitalized with a high-speed 16-channel acquisition device (wavebook 512A and wavebook 10A, IOtech) at a 10 kHz sampling rate. Fourteen channels, along with two channels dedicated to the continuous recording of respiratory signal and stimulus onset, were connected to the 14 lowest points on the electrode tip. Note that the two topmost recording points on the electrode were not used.

Odors and acquisition protocol

Odors were simple linear aliphatic compounds and either the main L or the F associated with this chain varied between odors. The odors used are listed in Table 1. Stimuli were delivered with a custom-made olfactometer at 1/6 of the saturation vapor pressure (SVp). The vaporized odors were injected in a constant and stable humidified airflow so that there were no variations in the overall flow; this was important, as we wanted to avoid any artifacts due to mechanical stimulation of the olfactory mucosa at odor onset and offset. Recording epochs were 15 s long and were sub-divided in three 5 s epochs corresponding to pre-stimulus basal activity, stimulus-related activity and post-stimulus activity, respectively.

Once the electrode was satisfactorily placed close to or within the mitral cell layer, stimulations were delivered in a regular sequence comprised of 15 s of recording, including 5 s of actual stimulation, and 90 s of rest. Within a sequence, odors with the exception of D07 were randomized. D07 was always delivered last, because the rinsing time for this odor is greater than 90 s. Preliminary experiments showed that the order of presentation had no effect on the recorded patterns (data not shown).

TABLE 1. Panel of odors used in this study

Carbon chain length (L)	Chemical function (F)	
	Designation	Symbol
Alcohol		
5	Pentanol	A05
6	Hexanol	A06
7	Heptanol	A07
10	Decanol	A10
Ester		
5	Ethyl-valerate	E05
6	Ethyl-hexanoate	E06
7	Ethyl-heptanoate	E07
10	Ethyl-decanoate	E10
Ketone		
7	2-heptanone	K07
Aldehyde		
7	Heptanal	D07

Indicated for each odorant are the official name in chemical nomenclature and the symbol used in this report.

Respiratory cycle recording and analysis

Respiration was recorded with a home-made monitoring device based on a fast response time thermodilution airflow sensor (bidirectional micro bridge mass airflow sensor, AWM 2000 family, Micro Switch Honeywell). This setup was extensively described by Roux *et al.* (2006). Briefly, the time dimension of the respiratory epochs (inspiration and expiration), which can differ from trial to trial, was converted into a phase dimension defined as $[-\pi,0]$ and $[0,\pi]$ for inspiration and expiration, respectively. The zero point was set to be the transition between inhalation and expiration. In contrast to time representation, the phase representation was common to all trials. Phase representation of the respiratory cycle was used as a normalized time basis to average olfactory neural events. Thus, the respiratory phase of any oscillatory event can be accurately evaluated and represents the time of occurrence of an event relative to the respiratory cycle.

LFP analysis

The LFPs present bursts of oscillations and are highly non-stationary events. They are not continuous in mammals and may vary in amplitude or shift in frequency. Additionally, they occur in several frequency bands and produce recordings that are often quite noisy. Therefore, we chose a method based on a wavelet transform of the signal that addresses the aforementioned characteristics of LFPs. As the method is extensively described by Roux *et al.* (2007), we give here only a brief summary.

Wavelet transform

The wavelet transform of a signal (Mallat, 1989) is the result of the convolution of the signal and a function of variable frequency (in our case, the Morlet wavelet) (Kronland-Martinet *et al.*, 1988). It yields a matrix of coefficients, T_Ψ, representing the frequency content of the signal. The T_Ψ matrix is then normalized to generate a time-scale energy density distribution matrix P_Ψ that is adjusted so that the overall sum of all elements in P_Ψ equals 1.

For visualization purposes, the P_Ψ matrices were converted into a time–frequency representation in which the energy density distribution was color coded. Because a high graphic resolution was not necessary, the P_Ψ matrices were computed from a filtered and under-sampled version of the raw signal (filter, 0–200 Hz; sampling rate, 200 Hz).

As the duration of respiratory cycles can change over time, time–frequency representations were resampled to fit the linearized respiratory cycles. Energy density was no longer represented as a function of time and frequency but instead as a function of respiratory phase and frequency. Several phase–frequency representations can be compared and averaged while preserving the temporal course of LFPs. However, this requires normalization of the energy in phase–frequency representations. Phase–frequency representations were normalized over the pre-stimulus period. Theoretical and practical aspects of time–frequency representations based on wavelet transforms have been described by Vialatte *et al.* (2007).

Wavelet ridge extraction: information about the oscillatory epochs

A particular application of wavelet analysis was implemented to extract the characteristics of the LFP bursts from the P_Ψ matrix. The analysis was performed in two steps. The first step involved a sweep of the low time-resolution coefficient matrix (i.e. the matrix computed from the under-sampled signal) for the detection of local maximum energy points, which correspond to the peaks of oscillatory activity. A threshold T_s was set for the detection of maxima to segregate signal from noise. T_s was defined as

$$T_s(f) = \overline{E(f)} + SD \cdot b, \tag{1}$$

where $E(f)$ is the averaged energy of the pre-stimulus period at frequency f, SD the SD of the same period and b an arbitrary constant (set to 6 in our case).

For each local maximum detected above the threshold, a higher resolution wavelet transform was then computed locally to detect the path of lowest energy decrease. This path was defined as the wavelet ridge. For each point (ϕ, f) of the ridge, we obtained instantaneous frequency and phase with $E(f) = T$. When the algorithm proceeded to a point at which $E(\phi, f_0) < T_s$ the detection process stopped. All extracted characteristics were stored in a MySQL engine database (MySQL AB). Several processing steps are summarized in Fig. 1 (top).

Data computation

After the LFP analysis step, all data were stored in a MySQL engine database. For each burst of oscillatory activity evoked by odor stimulation, the following parameters were stored: frequency, respiratory phase at the point of maximum energy and duration (expressed in radian, from 0 to 2π). Data with poor signal-to-noise ratios were eliminated. Wavelet ridge extraction was performed on the remaining recordings. As each burst was detected from the 14 recording points of the electrode, burst characteristics were averaged across the 14 points in the gamma or beta bands. Therefore, each individual odor stimulation was processed into a set of oscillation features comprising an average frequency, average duration and average respiratory phase. When the LFP oscillated in both bands, the set contained separate average values for each band. Data analysis was performed on 25 repetitions of the set of odors, recorded in 14 different animals (cf. Fig. 1). Some animals were
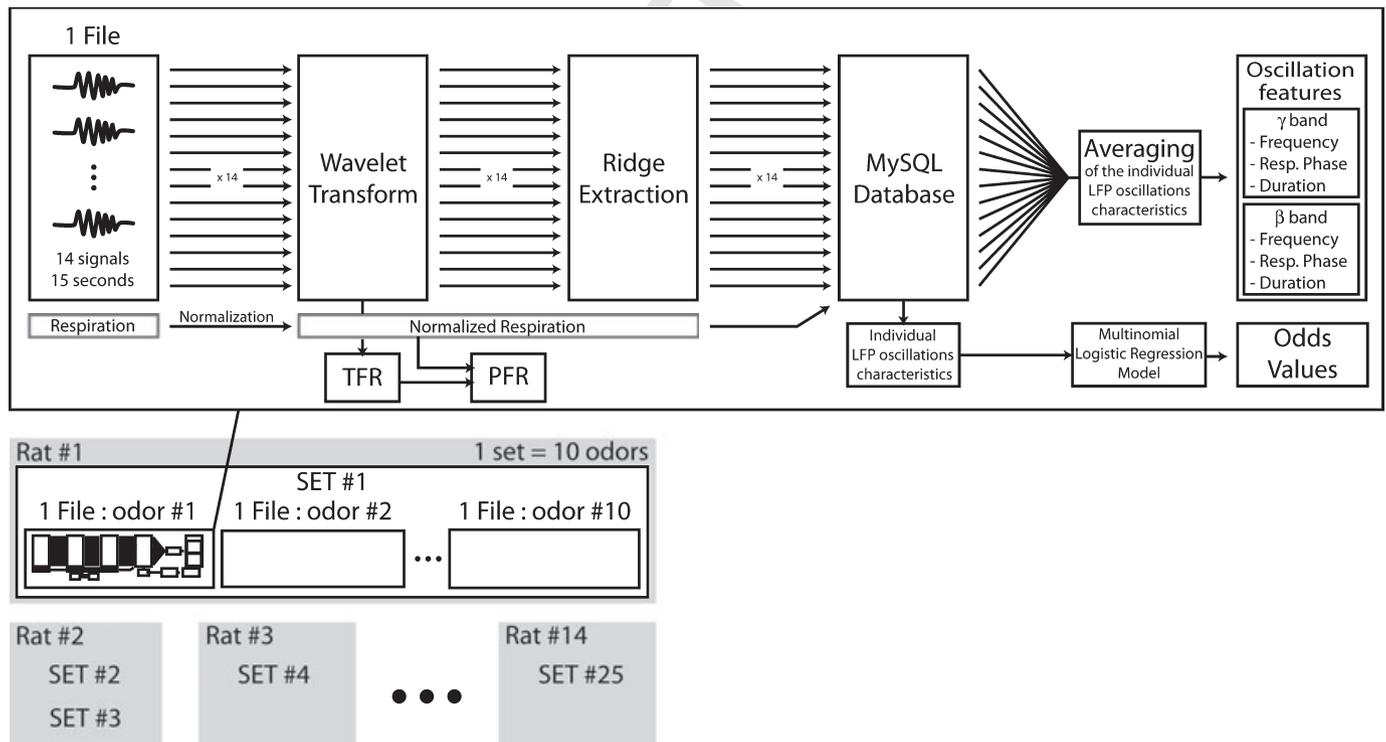

FIG. 1. From recording sessions to analysed results. Top: Signal-processing suite. From left to right: each file, which contains 14 signals from the 14 channels of the electrode plus the respiratory monitoring, undergoes several steps of data processing, including wavelet transform and ridge extraction. The results are stored in a database and visualized as time–frequency representations (TFRs). After normalization, the respiration is used to construct phase–frequency representations (PFRs) and measure the respiratory phase parameter. Each file produces a set of intrinsic oscillation features. All files are used both to obtain odds values and to construct a multinomial logistic regression model. Bottom: Organization of the recording sessions and data nomenclature. Each animal was used to record one or several sets; each set contains 10 files, each corresponding to one of the 10 odorants. A total of 25 sets were recorded from 14 different animals. From the resulting 250 files, 43 were eliminated because of noise or electrophysiological parasites.

used to record several sets of signals from different recording sites. The 25 sets are considered statistically independent. After LFP analysis and averaging, statistical analysis was performed for 207 sets of oscillation features.

Statistical analysis

Each odorant can be described via its F and L (see Table 1). Each set of oscillation features contains averaged LFP characteristics describing respiratory phase, duration and frequency. The variable F was qualitative, whereas L was quantitative. Therefore, each statistical unit involves both an odor and a set of oscillation features. All of the statistical analyses were performed using R (R: A Language & Environment for Statistical Computing, R Development Core Team, R Foundation for Statistical Computing, 2006) and SAS (SAS Institute Inc., SAS 9.1.3 Help and Documentation, Cary, NC, USA, SAS Institute Inc., 2000–04) statistical software. The aim was to study the relationship between the odors (F and L) and the oscillating burst characteristics (respiratory phase, duration and frequency).

First, we used the R k-means clustering technique (Hartigan & Wong, 1979) to cluster observations based on their frequencies. We obtained two burst groups, one with low frequency and one with high frequency. We have referred to these groups as beta and gamma bursts. Next, histograms were made with the R hist function to visualize the differences in the duration distribution between gamma and beta bursts. The same procedure was completed for the respiratory phase variable. To investigate if there were significant mean differences for the frequency, duration and respiratory phase variables between these two groups, we performed a MANOVA and ANOVA constructed from the whole data set, using the cluster factor (which corresponds to the classification of the bursts in the gamma or beta band or the k-means separation of the two clusters). A Fisher test was also applied to compare the variability of duration and respiratory phase for each group. Two other ANOVAS were conducted on the characteristics (frequency, duration and respiratory phase) of gamma and beta bursts, using odor identity as a factor.

Second, we used a multinomial logistic regression to explain the different observed oscillatory LFP patterns (Long, 1997). We performed this regression via the SAS CATMOD procedure and the explanatory variables were L and F. This model enabled us to compute the probability of obtaining a certain oscillatory pattern, given L and F. It was also possible to obtain the odds

$$\Omega_{i,j}(L,F) = \frac{P(pattern = i|L,F)}{P(pattern = j|L,F)}, \quad i,j = 1,2,3,$$

which gives the probability ratio *i pattern* : *j pattern* evoked by a specific odorant. In this framework, Wald and likelihood ratio tests were performed to examine effect significance and model validity. Finally, we calculated the correlation factor between odds values and SVp with R using the Pearson method.

Results

Twenty-five recording sessions were performed on 14 adult Wistar male rats. Each set gathered 10 recordings, with one recording per odor. After wavelet transform processing, files were averaged as described in Materials and methods. The following results were obtained through analysis of the 207 recording files.

TABLE 2. ANOVA summary: oscillation feature comparison between the two frequency bands

Comparisons and variables	Factor	F ratio	P-values
MANOVA	Cluster	$F_{2,533} = 95.206$	$P \ll 0.001$***
ANOVA			
Fr	Cluster	$F_{2,533} = 600.82$	$P \ll 0.001$***
Ph	Cluster	$F_{2,533} = 4.999$	$P = 0.0071$**
Du	Cluster	$F_{2,533} = 178$	$P \ll 0.001$***

Influence of the cluster factor on the frequency (Fr), duration (Du) and respiratory phase (Ph) characteristics of the odor-evoked LFP oscillations. Significance levels are indicated with standard annotations (ns > 5% > * > 1% > ** > 0.1% > ***). The cluster factor corresponds to the clusters defined by the k-means tool.

Molecular features do not determine the intrinsic characteristics of LFP oscillations

Odor-evoked LFP oscillations are characterized by their oscillatory frequency, duration and respiratory phase. Based on their oscillatory frequency, we distinguished two categories of bursts: fast bursts referred to as gamma oscillations, with frequency ranging from 40 to 80 Hz, and slow bursts referred to as beta oscillations, with frequency ranging from 10 to 35 Hz. Objective classification into beta or gamma categories was performed using the k-means clustering tool. Using this classification as a factor (designated as 'cluster factor'), an ANOVA was performed on the characteristics of the bursts. The results shown in Table 2 reveal that bursts classified as beta or gamma may also be sorted based on their duration and respiratory phase values. The characteristics of beta and gamma bursts are illustrated in Fig. 2. Bursts in the gamma band are characterized by a short duration and a respiratory phase mainly centred around 0, which indicates that these bursts occur mainly at the transition between inspiration and expiration. Conversely, bursts in the beta band are characterized by a long duration and a significantly variable respiratory phase (Fisher test, *P*-value $\ll 0.001$).

We then analysed the effect of the 'odor identity' factor on the characteristics of the bursts (ANOVA, cf. Table 3). Within the gamma range, odor had no influence on any of the characteristics. However, in the beta range, the respiratory phase of the bursts appears to vary significantly with the odor factor. This accounts for the variability in respiratory phase characterizing beta bursts in Fig. 2. In conclusion, the only oscillation intrinsic feature varying with odor is the respiratory phase of beta oscillations.

Odor quality determines the temporal patterning of bulbar oscillations

We showed that different odors evoke LFP bursts with very little variation in their intrinsic characteristics. However, it appeared that different odors induced oscillations in the beta and/or gamma ranges with different probabilities. Earlier studies (Buonviso *et al.*, 2003, 2006) reported that the two oscillatory regimes were related to the breathing cycle in an alternating fashion (Fig. 3a and b). Gamma oscillations occur around the transition between inspiration and expiration, whereas beta oscillations occur primarily during expiration and its subsequent plateau. The use of a large set of odorants in this study allowed us to observe a temporal pattern of LFP oscillations that we did not describe in our previous studies. An example of such a pattern is presented in Fig. 3b. Surprisingly, the
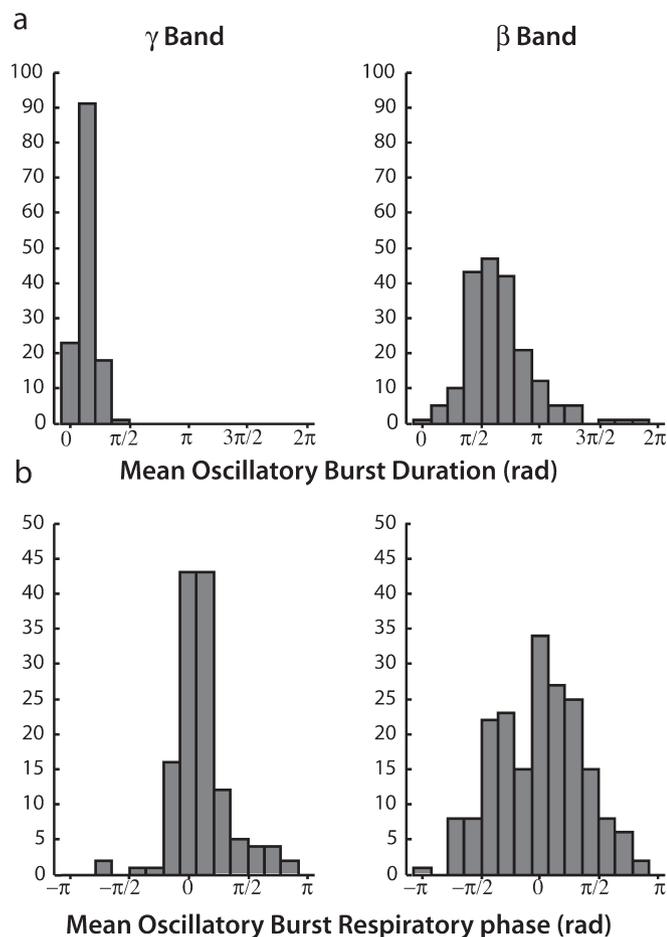
FIG. 2. Intrinsic oscillation feature comparison between the two frequency bands. (a) Distribution of oscillatory burst durations in the gamma (left) and beta (right) bands. This analysis is based on non-averaged LFP characteristics, regardless of the odorant used for the stimulation. Oscillations in the gamma band are highly reproducible and characterized by a short duration. (b) Distribution of respiratory phase of the gamma (left) and beta (right) bursts. Phase 0 corresponds to the transition between inspiration and expiration. The respiratory phase of beta oscillations is spread out over the entire respiratory cycle.

TABLE 3. ANOVA summary: molecular features do not determine the intrinsic characteristics of LFP oscillations

ANOVA variable	Factor	F ratio	P-value
Gamma band			
Fr	Odor	$F_{9,115} = 1.032$	n.s.
Ph	Odor	$F_{9,115} = 1.136$	n.s.
Du	Odor	$F_{9,115} = 1.179$	n.s.
Beta band			
Fr	Odor	$F_{9,181} = 1.659$	n.s.
Ph	Odor	$F_{9,181} = 2.186$	0.025*
Du	Odor	$F_{9,181} = 1.212$	n.s.

Influence of the odor identity factor on the intrinsic characteristics of odor-evoked bursts elicited in the gamma and beta ranges. Gamma bursts appear not to vary with the odor. The odor identity factor does have a significant effect on the respiratory phase (Ph) of odor-evoked bursts in the beta range. Significance levels are indicated with standard annotations (ns > 5% > * > 1%). Du, duration; Fr, frequency.

pattern is mainly characterized by a lack of activity in the gamma band and an occasional shift in the respiratory phase of the beta bursts.

Although both patterns could be observed in response to stimulation by any given odor from our set, we observed a strong predominance of this latter pattern in response to odors containing the alcohol chemical group. Faced with this observation, we formulated the hypothesis that the chemical features of odors may influence the temporal pattern of LFP oscillatory activity. To test this hypothesis, we used our data as a basis to construct a statistically valid model of the odor-related patterning of bulbar oscillations. This model was then used to predict the probability that an odor would elicit any one of the following three oscillatory patterns: (i) alternating bursts of gamma and beta oscillations (standard pattern); (ii) beta oscillatory bursts with no activity in the gamma band (gammaless pattern); or (iii) gamma oscillatory bursts with no activity in the beta band (betaless pattern). Figure 4 shows the model's predictions for the probability of each available combination of L and chemical F eliciting the three LFP patterns. It appears that the probability for each pattern (standard, betaless and gammaless) varies with F and L. A Wald test was used to evaluate the significance of the model. It yielded a P-value of 0.05 for the L factor and a P-value less than 0.001 for the F factor. The two leftmost columns in Fig. 4 show the variations in pattern probabilities related to the L for alcohol and ester molecules. As the L increases (from 5 to 10), so does the probability of eliciting a gammaless pattern. Conversely, the probability of eliciting a standard pattern decreases along this same interval. Hence, the results obtained from this model suggest that LFP patterns, if not precisely odor-specific, are still influenced by the chemical characteristics of odors. In a preliminary experiment, we compared the LFP patterns elicited in four distinct regions of the OB (antero-medial, antero-lateral, postero-medial and postero-lateral quadrants) by several odors. Data analysis revealed no significant difference in LFP activity between quadrants. We are therefore confident that the differences in patterns that we see here are related to odor features and not to recording site.

Odor vapor pressure determines the probability of gamma occurrence within the limits of a chemical family

The multinomial logistic regression revealed that odor identity, i.e. L/F pair, determines the probability of oscillation temporal patterning. However, a recent study has demonstrated that odor vapor pressure determines the range of oscillatory frequency (Lowry & Kay, 2007). Therefore, in a last step, we wanted to verify that the variations in temporal pattern that we observed were not simply due to differences in vapor pressure within our odor set. We proceeded as follows. We had to quantify the variation in oscillation temporal patterning induced by each odor. This was achieved by calculating an 'odds value' representing the ratio of the probability of eliciting the standard pattern over the probability of eliciting the gammaless pattern (beta and gamma/beta). Each odor is characterized by one and only one odds value reported in Fig. 4. An odds value less than 1 indicates that an odor displays a higher probability of eliciting a gammaless pattern than a standard pattern. As all odors were delivered at the same fraction of their SVp, we were able to test the correlation between the probability of an odor inducing gamma oscillations (odds values) and SVp of the odor. The correlation between odds values and SVp was determined with the inbuilt R function and evaluated with the Pearson test. If SVp were the only parameter determining the pattern, SVp and odds values should correlate perfectly. As illustrated in Fig. 5a, a good correlation ($r = 0.5$, Pearson P-value $\ll 0.0001$) was found between the two parameters. However, when odors are sorted into sub-groups (alcohol and ester groups), we found that SVp and odds values were more strongly correlated ($r = 0.9$ for each group, Pearson
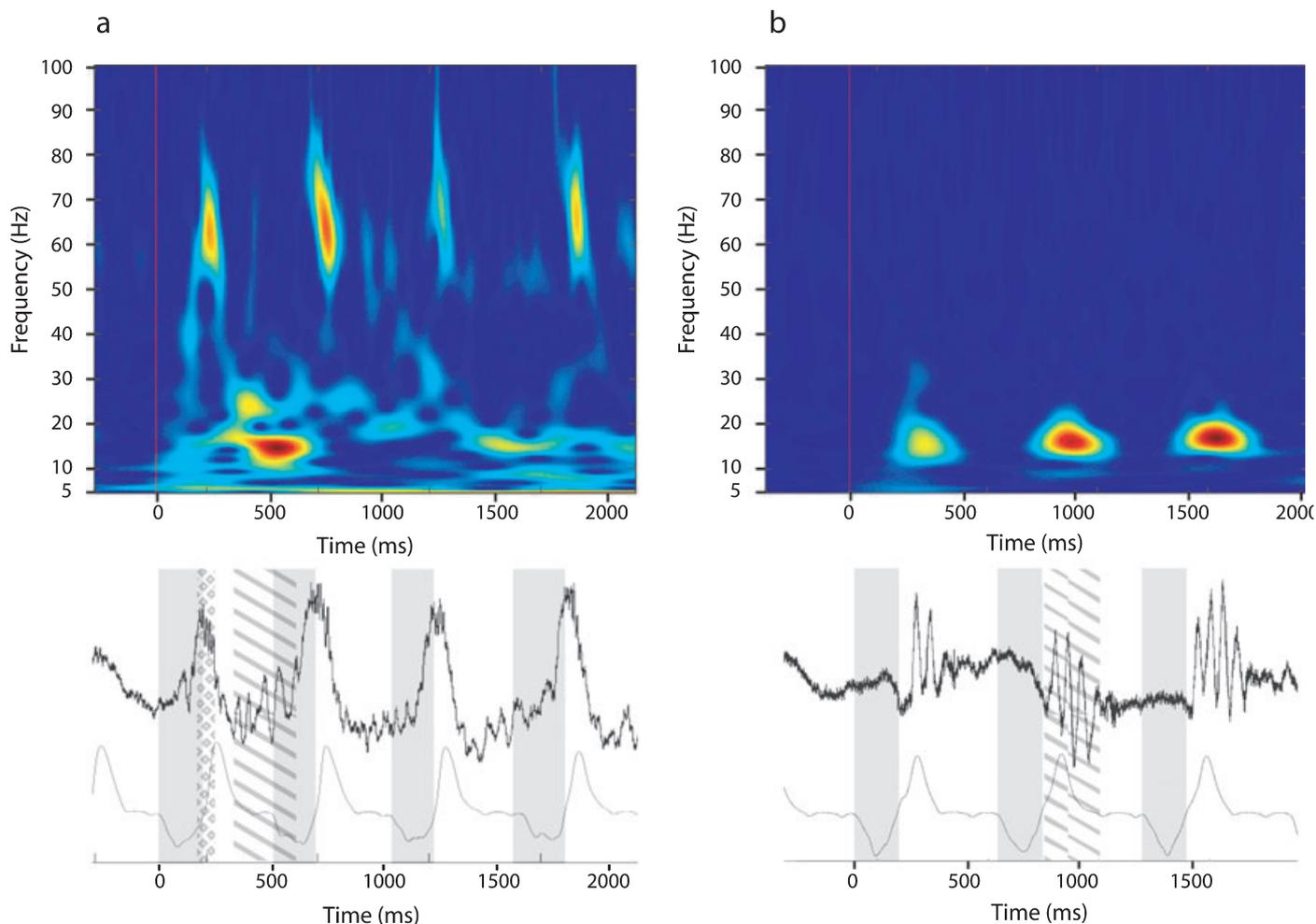
FIG. 3. Time–frequency representations (TFRs) of the standard and gammaless patterns. TFRs of bulbar LFP signals. Here, we presented only 2.5 s periods containing a short part of the pre-stimulus period and three or four respiratory cycles during stimulation. (a) Example of a standard pattern. Top: TFR obtained by wavelet transformation of the signal in response to stimulation with ester E05 (ethyl pentanoate). The vertical red bar indicates the onset of the stimulation and corresponds to time zero. The *y*-axis runs from 5 to 100 Hz. The standard pattern shows alternating epochs of oscillations in the beta and gamma bands. Energy is color coded: blue, low energy; red, high energy. Bottom: upper trace, raw signal. A diamond background indicates a gamma oscillation, whereas a striped background indicates a beta oscillation. Lower trace: respiration. Shaded and white areas correspond to inspiration and expiration phases, respectively. (b) Example of a gammaless pattern. TFR obtained by wavelet transformation of the signal in response to stimulation with alcohol A06 (hexanol). Note that the gammaless pattern shows strong bursts of oscillations in the beta band only. Same codes as in (a). Bottom: same legend as in (a).

P-value << 0.0001; Fig. 5b and c). Furthermore, a major difference appears between the two families: odds values for alcohols are always ≤ 1, whereas odds values for esters are always ≥ 1 (Fig. 5b and c). This means that alcohols have a high probability of evoking the gammaless pattern, whereas esters have a high probability of triggering the standard pattern. Taken together these results indicate that, for the same F, SVp determines the probability of gamma occurrence. This relation is no longer true for molecules with different Fs.

To illustrate the discontinuities between odds values and SVp values when odors belong to different families, we chose two examples. In Fig. 6a, odors (E07 vs. A06) elicit patterns of oscillations far more different than would be predicted from their close SVp values (124 and 91 Pa, respectively). The odds values for these two odors indicate that patterns would be quite dissimilar (odds values, A06 = 0.83, E07 = 1.78). The opposite case is illustrated in Fig. 6b. Despite having very dissimilar SVps (6 and 293 Pa), these two odors (E10 and A05, respectively) elicit very similar LFP patterns that are confirmed by their close odds values (E10 = 0.90; A05 = 1.04).

In conclusion, it seems that odor quality determines a range of possible odds values and that the SVp of the odor sets the definitive odds value of the odor.

Discussion

As previously described (Buonviso *et al.*, 2003), we observed that odors elicit oscillations in the LFPs that can be strictly separated in two categories based on several characteristics. The designation of these oscillations is based on their frequency, and thus we defined two bands designated as beta and gamma. We show here that bursts of oscillations could be separated effectively on the basis of their duration or respiratory phase. Statistical analysis revealed that odor has little influence over the intrinsic characteristics of the oscillations. With the exception of the respiratory phase of beta oscillations, oscillations remain constant regardless of odor identity. Conversely, odor identity has a strong influence on the temporal patterning of LFP oscillatory activity. Moreover, for molecules of the same chemical family, the probability of gamma occurrence is greatly correlated to
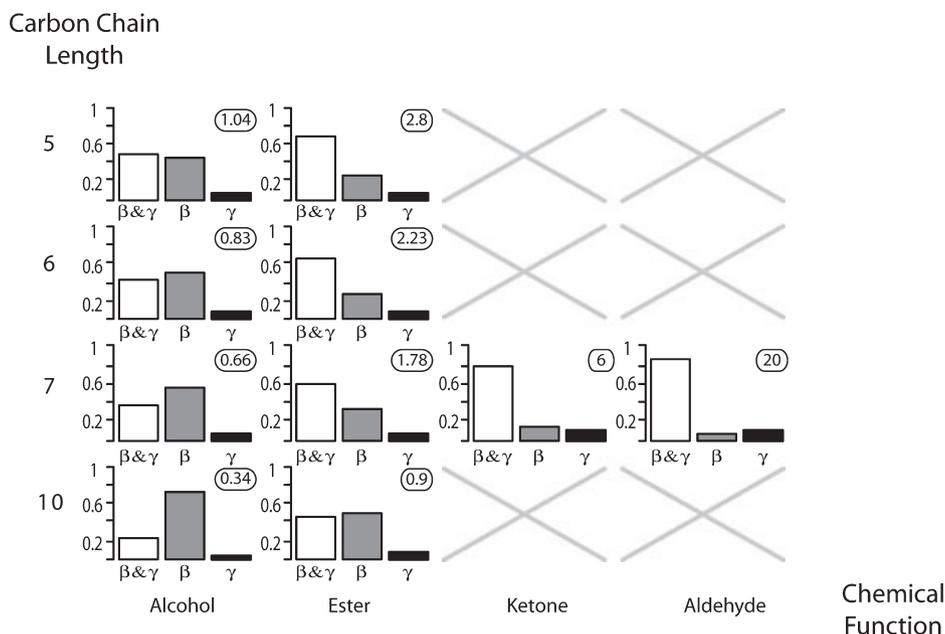
FIG. 4. Odor quality determines the temporal patterning of bulbar oscillations. Probability histograms for three patterns of oscillations: standard (beta and gamma, unfilled bars), gammaless (beta, grey bars) and betaless (gamma, black bars. The vertical scale indicates the probability of a pattern occurrence. All results presented here come from the model constructed from our experimental data. Histograms are ordered as a function of both L of the odor molecules (rows: from bottom to top 10, 7, 6 and 5 carbons) and molecular F (columns: A, E, K and D). The odds value associated with each molecule is indicated at the upper right corners.
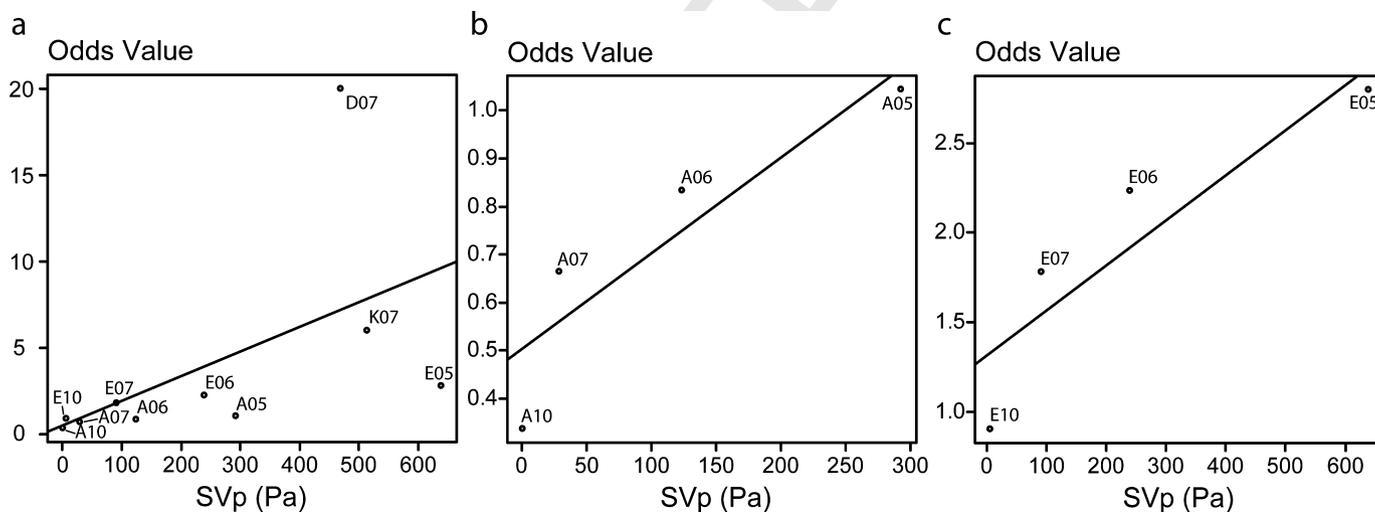

FIG. 5. Correlation between SVp and odds values. The SVp values were estimated with the EPI v3.11 (Estimation Programs Interface) software suite developed by the US Environmental Protection Agency's Office of Pollution Prevention Toxics and Syracuse Research Corporation. (a) Correlation for all odors used in the stimulation protocol, with first-degree best polynomial fit of equation $f(x) = 0.01436x + 0.46561$. Correlations within alcohol (b) and ester (c) chemical families, with first-degree best polynomial fit of equations $f(x) = 0.001998x + 0.501441$ and $f(x) = 0.002516x + 1.314804$, respectively.

odor vapor pressure. This correlation is not so strong for odors with different Fs.

Determination of temporal patterning by odorant features

Each molecule has the ability to elicit both standard patterns, which are characterized by alternating bursts in the gamma and beta bands, and gammaless patterns, which are characterized by beta oscillations alone, with different probabilities. The ratio between these two probabilities has been defined as an odor's odds value. For odors with a similar F (homologous series of alcohols or esters), odds values are correlated with the L of the molecule. For the same F, the longer the odor's carbon chain, the lower its SVp (volatility) and the lower its probability to evoke oscillations in the gamma range. As suggested by the recent work of Lowry & Kay (2007), SVp is a good estimator of the airborne concentration of the odor. In such conditions, we may assume that odds values within a chemical family are determined by the airborne concentration of the molecules. However, our data show that the correlation between odds values and SVp is greatly enhanced when odors belong to the same chemical family (see Fig. 5). Within
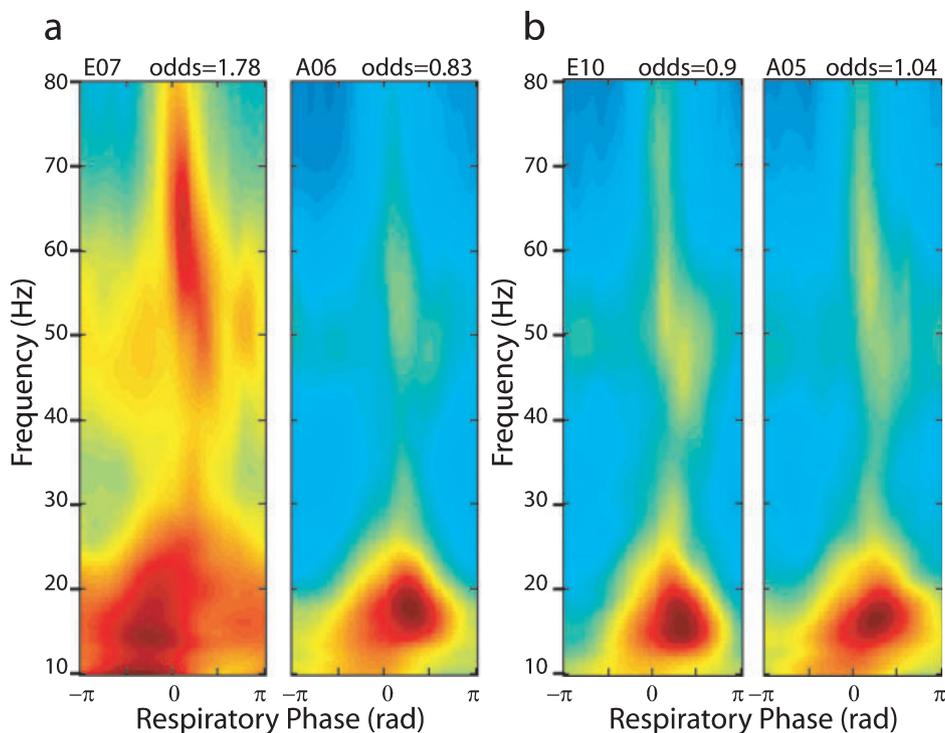
COLOUR

FIG. 6. Patterns of oscillations evoked by two pairs of odors. Phase–frequency representations of odor-evoked LFP patterns. All respiratory cycles from the stimulation epoch are averaged. Energy is color-coded: blue, low energy; red, high energy. Odds values are indicated at upper right corners. SVp values are as follows: E07, 91 Pa; A06, 124 Pa; E10, 6 Pa; A05, 293 Pa. (a) Two odors with dissimilar odds values induce dissimilar LFP patterns. E07 (left) evokes high energy in the gamma band with a negative beta respiratory phase. In contrast, A06 (right) evokes mainly beta oscillations with a positive respiratory phase. (b) Two odors with close odds values induce very similar LFP patterns, with little energy in the gamma band and a positive respiratory phase for beta oscillations.

two chemical families (alcohol and ester), the relationship between SVp and odds value is nearly linear and thus very comparable. A notable difference in these relationships lies in the fact that the overall odds value for alcohols is below 1, whereas the overall odds value for esters is above 1. This suggests that the chemical family determines a range of possible odds values and that the vapor pressure of the odor will set the definitive odds value of the odor in particular conditions. By setting the range in which the odds value will vary, the chemical family categorizes the odor at a very early stage of olfactory information processing.

Significance of different oscillatory frequency ranges

We observed that gamma oscillations, when they exist, occur with the same respiratory phase around the transition between inspiration and expiration. This phase corresponds to the moment of maximal amplitude on an electro-olfactogram (Chaput, 2000), which is probably also the time of maximal neuroreceptor activation. This observation led us to the hypothesis that gamma occurrence could be related to the time of maximal concentration in the olfactory epithelium, implying therefore that gamma oscillations would reflect a high afferent input excitation. The observation that beta waves occur mainly during expiratory epochs when the concentration of the odorant molecule is lower in the olfactory epithelium supports this assumption. This interpretation is in agreement with the report of Neville & Haberly (2003) that odors at high concentrations induced prominent gamma frequency oscillations, whereas those at lower concentrations elicited beta oscillations. However, in waking animals, high power in the beta spectrum is obtained in response to highly volatile odors (Lowry & Kay, 2007). This discrepancy might be

explained by the sniffing behavior of the animal, which could produce a different influx of molecules into the nasal cavity.

We observed in our study that aliphatic alcohols mostly elicited LFP patterns characterized by a lack of gamma oscillations. According to the preceding discussion, the assumption can be made that odors inducing gammaless patterns are composed of molecules that poorly activate the olfactory epithelium. Such a poor activation may originate from different circumstances, e.g. (i) low airborne concentration of the odor in the nasal cavity (possibly linked to a low SVp); (ii) low number of receptor neurons tuned to the odor; (iii) difficult access to the receptor site; or (iv) low solubility and/or high hydrophobicity. This hypothesis finds support in a recent report showing that electro-olfactogram response modulation by sniff rate and decay time varies with molecular odorant features (Scott *et al.*, 2006).

Functional relevance

Our results can be compared with those from the optical imaging of intrinsic signals obtained by Uchida *et al.* (2000). Indeed, these authors report that odor receptors possessing a common molecular-feature receptive site are grouped together and represented by glomeruli that are localized in topographically fixed domains in the OB. Various structural features differentially influence the spatial map of activated glomeruli. The F has been designated as the 'primary feature' of the molecule and the L has been designated as a 'secondary feature.' The former characterizes a domain of activated glomeruli in the spatial map and the latter represents the local arrangement of activated glomeruli within the domain. Moreover, a domain exhibits a polarity such that a systematic and gradual shift of the positions of

activated glomeruli occurs with an increase in the L of odors. Thus, a parallel can be drawn as follows: the 'primary feature', or F, determines both the domain in glomerular maps and the odds value range in our data. The 'secondary feature', or L, determines the local position in the glomerular map and the evolution of odds values within the range determined by the chemical family. This last statement is in agreement with our observation that a relationship exists between odds value and SVp within a chemical family. The concept could be refined by introducing supplemental features, each of which describes a molecular property. It is the sum of all features that will ultimately determine the elicited pattern of oscillations.

From a functional point of view, it is plausible that the molecular features of the odors (steric size, solubility, number of double bonds, etc.) define the pattern of neuroreceptor activation. Peripheral activation can be assumed to evoke an odor-specific glomerular spatial map that is converted into an odor-specific spatio-temporal map of oscillatory LFP activity. The exact role that the LFP may play in information coding is as yet unknown but several studies suggest that the LFP reflects synaptic, rather than spiking, activity. Thus, LFPs could provide a temporal frame, underlying and pacing the spiking activity, that would vary with olfactory stimulus characteristics. The importance of LFPs lies in the possibility that they may structure the time dimension of bulbar output. Therefore, temporal structuring of bulbar output might reflect the molecular features of an odor, including both its chemical family and its more precise identity within the family. This view is supported by the report from Friedrich *et al.* (2004), which reveals a simultaneous conveyance of both odor category and identity by the same population of zebrafish bulbar neurons, a multiplexing strategy based on a double time-scale reading. The temporal frame provided by LFP oscillations may be involved in a similar strategy in the rat OB.

Acknowledgements

Abbreviations

F, functional group; L, carbon-chain length; LFP, local field potential; OB, olfactory bulb; SVp, saturation vapor pressure.

References

Belluscio, L. & Katz, L.C. (2001) Symmetry, stereotypy, and topography of odorant representations in mouse olfactory bulbs. *J. Neurosci.*, **21**, 2113–2122.

Buck, L. & Axel, R. (1991) A novel multigene family may encode odorant receptors: a molecular basis for odor recognition. *Cell*, **65**, 175–187.

Buonviso, N. & Chaput, M.A. (1990) Response similarity to odors in olfactory bulb output cells presumed to be connected to the same glomerulus: electrophysiological study using simultaneous single-unit recordings. *J. Neurophysiol.*, **63**, 447–454.

Buonviso, N., Chaput, M.A. & Berthommier, F. (1992) Temporal pattern analyses in pairs of neighboring mitral cells. *J. Neurophysiol.*, **68**, 417–424.

Buonviso, N., Amat, C., Litaudon, P., Roux, S., Royet, J., Farget, V. & Sicard, G. (2003) Rhythm sequence through the olfactory bulb layers during the time window of a respiratory cycle. *Eur. J. Neurosci.*, **17**, 1811–1819.

Buonviso, N., Amat, C. & Litaudon, P. (2006) Respiratory modulation of olfactory neurons in the rodent brain. *Chem. Senses*, **31**, 145–154.

Chaput, M.A. (2000) EOG responses in anesthetized freely breathing rats. *Chem. Senses*, **25**, 695–701.

Friedrich, R.W. & Laurent, G. (2001) Dynamic optimization of odor representations by slow temporal patterning of mitral cell activity. *Science*, **291**, 889–894.

Friedrich, R.W., Habermann, C.J. & Laurent, G. (2004) Multiplexing using synchrony in the zebrafish olfactory bulb. *Nat. Neurosci.*, **7**, 862–871.

Hallem, E.A. & Carlson, J.R. (2006) Coding of odors by a receptor repertoire. *Cell*, **125**, 143–160.

Hartigan, J.A. & Wong, M.A. (1979) A K-means clustering algorithm. *Appl. Stat.*, **28**, 100–108.

Imamura, K., Mataga, N. & Mori, K. (1992) Coding of odor molecules by mitral/tufted cells in rabbit olfactory bulb. I. Aliphatic compounds. *J. Neurophysiol.*, **68**, 1986–2002.

Johnson, B.A., Woo, C.C. & Leon, M. (1998) Spatial coding of odorant features in the glomerular layer of the rat olfactory bulb. *J. Comp. Neurol.*, **393**, 457–471.

Jourdan, F., Duveau, A., Astic, L. & Holley, A. (1980) Spatial distribution of [14C]2-deoxyglucose uptake in the olfactory bulbs of rats stimulated with two different odours. *Brain Res.*, **188**, 139–154.

Katoh, K., Koshimoto, H., Tani, A. & Mori, K. (1993) Coding of odor molecules by mitral/tufted cells in rabbit olfactory bulb. II. Aromatic compounds. *J. Neurophysiol.*, **70**, 2161–2175.

Kronland-Martinet, R., Morlet, J. & Grossman, A. (1988) Analysis of sound patterns through wavelet transforms. *Int. J. Patt. Rec. Art. Intell.*, **1** (2), 273–301.

Long, J.S. (1997) *Regression Models for Categorical and Limited Dependent Variables (Advanced Quantitative Techniques in the Social Sciences)*. Sage Publications, Thousand Oaks, CA.

Lowry, C.A. & Kay, L.M. (2007) Chemical factors determine olfactory system beta oscillations in waking rats. *J. Neurophysiol.*, **VV**, xxx–xxx. In press.

Mallat, S. (1989) A theory for multiresolution signal decomposition: the wavelet representation. *IEEE Trans. Patt. Anal. Mach. Intell.*, **11**, 674–693.

Malnic, B., Hirono, J., Sato, T. & Buck, L.B. (1999) Combinatorial receptor codes for odors. *Cell*, **96**, 713–723.

Martin, C., Gervais, R., Hugues, E., Messaoudi, B. & Ravel, N. (2004) Learning modulation of odor-induced oscillatory responses in the rat olfactory bulb: a correlate of odor recognition? *J. Neurosci.*, **24**, 389–397.

Mombaerts, P., Wang, F., Dulac, C., Chao, S.K., Nemes, A., Mendelsohn, M., Edmondson, J. & Axel, R. (1996) Visualizing an olfactory sensory map. *Cell*, **87**, 675–686.

Mori, K., Kishi, K. & Ojima, H. (1983) Distribution of dendrites of mitral, displaced mitral, tufted, and granule cells in the rabbit olfactory bulb. *J. Comp. Neurol.*, **219**, 339–355.

Mori, K., Mataga, N. & Imamura, K. (1992) Differential specificities of single mitral cells in rabbit olfactory bulb for a homologous series of fatty acid odor molecules. *J. Neurophysiol.*, **67**, 786–789.

Mori, K., Takahashi, Y.K., Igarashi, K.M. & Yamaguchi, M. (2006) Maps of odorant molecular features in the mammalian olfactory bulb. *Physiol. Rev.*, **86**, 409–433.

Neville, K.R. & Haberly, L.B. (2003) Beta and gamma oscillations in the olfactory system of the urethane-anesthetized rat. *J. Neurophysiol.*, **90**, 3921–3930.

Rall, W., Shepherd, G.M., Reese, T.S. & Brightman, M.W. (1966) Dendro-dendritic synaptic pathway for inhibition in the olfactory bulb. *Exp. Neurol.*, **14**, 44–56.

Roux, S.G., Garcia, S., Bertrand, B., Cenier, T., Vigouroux, M., Buonviso, N. & Litaudon, P. (2006) Respiratory cycle as time basis: an improved method for averaging olfactory neural events. *J. Neurosci. Meth.*, **152**, 173–178.

Roux, S.G., Cenier, T., Garcia, S., Litaudon, P. & Buonviso, N. (2007) A wavelet-based method for local phase extraction from a multi-frequency oscillatory signal. *J. Neurosci. Meth.*, **160**, 135–143.

Rubin, B.D. & Katz, L.C. (1999) Optical imaging of odorant representations in the mammalian olfactory bulb. *Neuron*, **23**, 499–511.

Scott, J.W., Acevedo, H.P. & Sherrill, L. (2006) Effects of concentration and sniff flow rate on the rat electroolfactogram. *Chem. Senses*, **31**, 581–593.

Shepherd, G.M. & Greer, C.A. (1998) Olfactory bulb. In Shepherd, G.M. (Ed.), *The Synaptic Organization of the Brain*. Oxford UP, NY, pp. 159–203.

Stopfer, M., Bhagavan, S., Smith, B.H. & Laurent, G. (1997) Impaired odour discrimination on desynchronization of odour-encoding neural assemblies. *Nature*, **390**, 70–74.

Uchida, N., Takahashi, Y.K., Tanifuji, M. & Mori, K. (2000) Odor maps in the mammalian olfactory bulb: domain organization and odorant structural features. *Nat. Neurosci.*, **3**, 1035–1043.

Vassar, R., Chao, S.K., Sitcheran, R., Nuñez, J.M., Vosshall, L.B. & Axel, R. (1994) Topographic organization of sensory projections to the olfactory bulb. *Cell*, **79**, 981–991.

Vialatte, F.B., Martin, C., Dubois, R., Haddad, J., Quenet, B., Gervais, R. & Dreyfus, G. (2007) A machine learning approach to the analysis of time-frequency maps, and its application to neural dynamics. *Neural Netw.*, **20**, 194–209.

Wehr, M. & Laurent, G. (1996) Odour encoding by temporal sequences of firing in oscillating neural assemblies. *Nature*, **384**, 162–166.

Willhite, D.C., Nguyen, K.T., Masurkar, A.V., Greer, C.A., Shepherd, G.M. & Chen, W.R. (2006) Viral tracing identifies distributed columnar organization in the olfactory bulb. *Proc. Natl Acad. Sci. U.S.A.*, **103**, 12 592–12 597.

Zhao, H., Ivic, L., Otaki, J.M., Hashimoto, M., Mikoshiba, K. & Firestein, S. (1998) Functional expression of a mammalian odorant receptor. *Science*, **279**, 237–242.

Author Query Form

Dear Author,
During the copy-editing of your paper, the following queries arose. Please respond to these by marking up your proofs with the necessary changes/additions. Please write your answers on the query sheet if there is insuicient space on the page proofs. Please write clearly and follow the conventions shown on the attached corrections sheet. If returning the proof by fax do not write too close to the paper's edge. Please remember that illegible mark-ups may delay publication.

Many thanks for your assistance.

Query reference	Query	Remarks
1	Au: Is short running title OK?	
2	Please also give name of ethical committee which approved the study.	
3	Au: **Kronland-Martinet 1988** has been changed to **Kronland-Martinet *et al.* 1988** so that this citation matches the list	
4	Au: 'in that' $\rightarrow$ 'in the possibility that'. OK?	
5	Au: Jonhson $\rightarrow$ Johnson. OK?	
6	Au: Lowry: Please check year (here and in text) and supply volume no. and page extent	
7	Please define "*" in Table 2	

MARKED PROOF

Please correct and return this set

Please use the proof correction marks shown below for all alterations and corrections. If you wish to return your proof by fax you should ensure that all amendments are written clearly in dark ink and are made well within the page margins.

Instruction to printer	Textual mark	Marginal mark
Leave unchanged	··· under matter to remain	(✓)
Insert in text the matter indicated in the margin	⅄	New matter followed by ⅄ or ⅄⊗
Delete	/ through single character, rule or underline or ⊢——⊣ through all characters to be deleted	⊘/ or ⊘/⊗
Substitute character or substitute part of one or more word(s)	/ through letter or ⊢——⊣ through characters	new character / or new characters /
Change to italics	— under matter to be changed	⌣
Change to capitals	≡ under matter to be changed	≡
Change to small capitals	= under matter to be changed	=
Change to bold type	∿ under matter to be changed	∿
Change to bold italic	≈ under matter to be changed	≈
Change to lower case	Encircle matter to be changed	⧣
Change italic to upright type	(As above)	⊥
Change bold to non-bold type	(As above)	⊥
Insert 'superior' character	/ through character or ⅄ where required	Y or ⅄ under character e.g. Y² or ⅄²
Insert 'inferior' character	(As above)	⅄ over character e.g. ⅄₂
Insert full stop	(As above)	⊙
Insert comma	(As above)	,
Insert single quotation marks	(As above)	Y or ⅄ and/or Y or ⅄
Insert double quotation marks	(As above)	Y or ⅄ and/or Y or ⅄
Insert hyphen	(As above)	⊢⊣
Start new paragraph	⌐	⌐
No new paragraph	↪	↪
Transpose	⊔⊓	⊔⊓
Close up	linking ⌣ characters	⌒
Insert or substitute space between characters or words	/ through character or ⅄ where required	Y
Reduce space between characters or words	│ between characters or words affected	↑